



HYDROTHERMALLY GROWN ZEOLITE CRYSTALS

*S. K. DURRANI, A. H. QURESHI, M.A. HUSSAIN, M. AHMAD¹, N. AHMED and N.K. QAZI

Materials Division, Directorate of Technology, PINSTECH, P.O. Nilore, Islamabad, Pakistan

¹ Physics Division, Directorate of Science, PINSTECH, P.O. Nilore, Islamabad, Pakistan

(Received December 17, 2008 and accepted in revised form February 24, 2009)

The aluminium-deficient and ferrosilicate zeolite-type materials were synthesized by hydrothermal process at 150-170°C for various periods of time from the mixtures containing colloidal reactive silica, sodium aluminate, sodium hydroxide, iron nitrate and organic templates. Organic polycation templates were used as zeolite crystal shape modifiers to enhance relative growth rates. The template was almost completely removed from the zeolite specimens by calcination at 550 °C for 8h in air. Simultaneous thermogravimetric (TG) and differential thermal analysis (DTA) was performed to study the removal of water molecules and the amount of organic template cations occluded inside the crystal pore of zeolite framework. The ~12-13% weight loss in the range of (140-560°C) was associated with removal of the $(C_3H_7)_4N^+$ cation and water molecules. X-ray diffraction (XRD) analysis and scanning electron microscope (SEM) techniques were employed to study the structure, morphology and surface features of hydrothermally grown aluminium-deficient and ferrosilicate zeolite-type crystals. In order to elucidate the mode of zeolite crystallization the crystallinity and unit cell parameters of the materials were determined by XRD, which are the function of Al and Fe contents of zeolites.

Keywords: Aluminium-deficient zeolite, ZSM-11, ZSM11-Fe, XRD and SEM, Particle size distribution.

1. Introduction

Zeolites are an important class of technological materials that are used in a wide variety of industrial applications including ion exchange, catalysts, membrane separation, nuclear waste disposal, chemical sensing, water treatment, gas separation & purification, liquid phase separation, molecular sieves, detergency, fertilizer, desiccation, soil improvers, animal feed supplements, pollution abatement, as nonlinear optical materials, hosts for semiconductor quantum dots and molecular wires [1-3]. The best-known members are composed of aluminosilicate framework of tetrahedral units of SiO_4 and AlO_4 , each tetrahedral unit linked by an oxygen atom [4] with channel and cage dimensions ranging between 0.2 and 2.0 nm, although frameworks with various other elements such as P, Ga, B, Zn, and transition metals can also be made [5]. Recently, synthetic zeolites are used commercially more often than natural zeolites due to the purity of crystalline products and the uniformity of particle sizes. Moreover, syntheses can be carried out using rather inexpensive starting materials. Typical synthesis of these materials is done via sol-gel and hydrothermal methods and involves rapid formation of an insoluble gel-like material with quaternary organic

template compounds from which the crystals emerge [6]. There is considerable interest in understanding the fundamental steps involved in the nucleation and crystal growth processes. Hydrothermal method is a "soft solution chemical processing" which provides an easy route to prepare a well-crystalline oxide at low temperature and short reaction time [7-9]. The evolution of the behavior of synthesized materials depends heavily on the structural information obtained from a wide range of physical methods traditionally used in materials chemistry. Knowledge of the crystallinity in molecular sieve matrix is required to assess their quality and its vital importance in catalytic reactions, especially in synthetic-fuel and petrochemical processing [10]. Various techniques have been used for characterization of crystallinity and microstructural properties of zeolite and zeotype materials include: Thermal analysis (TG/DTA), Fourier transform infrared (FTIR) spectroscopy, X-ray diffraction (XRD), X-ray absorption fine structure (XAFS), Raman spectroscopy, scanning electron microscope (SEM) and transmission electron microscopy (TEM) [11-13]. The present work deals with determination of percent crystallinity, microstructural features and particle size distribution of sol-gel and hydrothermally grown

* Corresponding author : durransk@gmail.com

high siliceous aluminium-deficient and ferrosilicate zeolite-type materials using TG/DTA, XRD, SEM techniques.

2. Experimental

2.1. Materials and synthesis

All chemicals used were of analytical reagent grade and used without further purification. Sodium silicate (27% silica from Aldrich), reactive silica (from alkaline extract of dry rice husk) [14], colloidal silica sol (Lodux-HS40, from Dupont 40% SiO₂) and sodium aluminate (32.6% Na₂O, 35.7% Al₂O₃ from Aldrich) were used as sources of silica

and alumina respectively. Tetrapropylammomium bromide (TPABr) and tetrabutylammonium bromide (TBABr), were used as organic template. Sodium hydroxide (from Fluka) was used for alkali metal cation. Homogeneous gel is formed by mixing of silica, inorganic salts, and organic template as mentioned in Table 1. Hydrothermal synthesis for aluminium-deficient and ferrosilicate zeolite specimens was conducted in polytetrafluoroethylene (PTFE)-lined stainless steel digestion bomb. Schematic representation of hydrothermal process is given in Fig. 1. In a typical hydrothermal synthesis of zeolite either ZSM11-Al or ZSM11-Fe, a solution-A was prepared by dissolving sodium

Table 1. Molar composition and hydrothermal conditions for synthesis of Aluminium-deficient and ferrosilicate zeolite-type materials.

Hydrothermal Conditions	Identification of Specimens					
	Aluminium-deficient-ZSM11			Ferro-ZSM11		
	ZA-1	ZA-2	ZA-3	ZF-1	ZF-2	ZF-3
Temperature (°C)	150	160	170	150	160	170
Time (Hours)	72	48	24	72	48	24
pH	10.35	10.75	11.15	11.00	11.35	11.75
Gel composition (Molar ratios)						
SiO ₂ /(TBA) ₂ O	8.65	8.33	7.76	16.75	20.09	27.65
H ₂ O /Na ₂ O	82.50	123.21	134.82	212.1	151.42	113.65
H ₂ O/SiO ₂	25.62	26.33	27.42	56.97	49.58	34.49
SiO ₂ /Al ₂ O ₃	92.15	117.23	122.14			
Al ₂ O ₃ /(TBA) ₂ O	0.094	0.071	0.063			
SiO ₂ /Fe ₂ O ₃				9.51	10.56	12.27
Fe ₂ O ₃ /(TBA) ₂ O				1.76	1.96	2.25

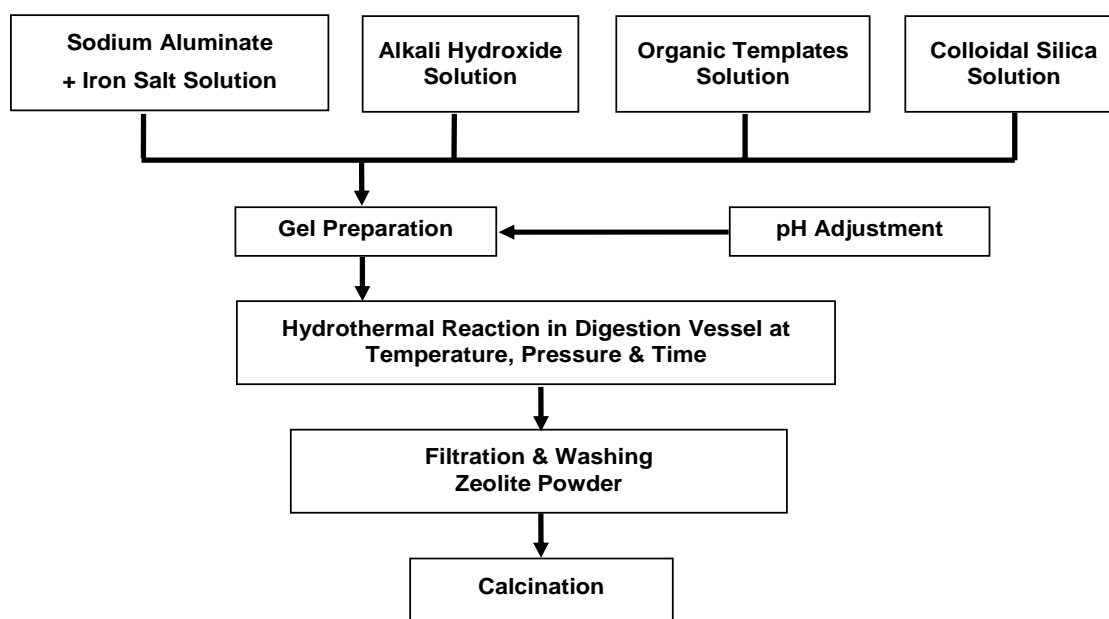


Figure 1. Hydrothermal process for synthesis of aluminum deficient or ferrosilicate zeolite-type materials.

aluminate, NaOH and Fe (NO₃)₃·9H₂O in deionized water and stirred until it becomes homogeneous. This solution was slowly added to silica solution (solution-B) containing TBABr and the reaction mixture was stirred until homogeneous gel was obtained. The gel was transferred in PTFE-lined digestion bomb and was aged hydrothermally in an oven maintained at 150-170 °C for various period of time (24-72 hours), after which the digestion bomb was quenched and the resulting solid and liquid phases were decanted. The liquid was retained for analysis. The solid product was washed with copious amounts of deionized water, dried in air at 100 °C in static oven and sieved, if necessary. Calcination of materials was conducted for 16 hours in shallow bed conditions at 550 °C.

2.2. Characterization

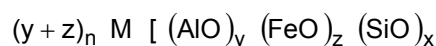
The elemental composition of zeolite specimens (ZA1-3 and ZF1-3) were measured by inductively coupled plasma (ICP-OES) spectrometer and electron probe micro analyzer attached with SEM. Silicon analysis of each zeolite specimen was determined gravimetrically as pure silica. The crystallinity and phase analysis of materials were conducted by X-ray diffraction using Rigaku Geiger flux instrument with CuK_α radiation (λ = 0.154056 nm). The XRD data were collected in the 2θ range from 15° < 2θ < 80° by step-scanning 0.5° increments and scanning rate of 5°/min. Various micro-structural features of aluminium-deficient and ferrosilicate zeolite-type materials were observed by scanning electron microscope (SEM) LEO 440I. The sample for SEM observation was prepared by 10 min ultrasonic dispersion of a small amount of sample in ethanol

and drop of the solution was put onto aluminum stud and dried in air. The specimen was coated with a thin film of evaporated gold. The organic template contents and water molecules were measured by thermogravimetric (TG) and differential thermal analysis (DTA) using simultaneous thermal analyzer Netzsch STA-409. Samples were scanned from 30 to 900 °C in air at a flow rate of 200ml min⁻¹ and heating rate of 10 °C min⁻¹. The average crystal size and particle size distribution was estimated by dynamic laser light scattering particle size analyzer (SK-Laser Micron PRO-7000S).

3. Results and Discussion

3.1. Chemical analysis

The hydrothermally synthesized zeolite-type materials were obtained in pure white powder form except the iron containing materials which were to some extent in brownish colour. Table 2 shows the results of chemical analysis and density of aluminium-deficient and ferrosilicate powder materials determined by classical chemical and instrumental methods [15-17]. The unit cell formulae were determined by chemical analysis of Al, Fe and Na using the following chemical product.



It was assumed that the number of Si + Al + Fe atoms per unit cell (x+y+z) was 96 for zeolite ZSM11 and n is the valance of the compensating cation M, as proposed by Kokotailo [18]. The results of Table 2 revealed that all the six synthesized specimens were ZSM-11 type zeolite

Table 2. Physico-chemical analysis of zeolite-type materials.

Specimens	%Weight Oxides			%Weight Loss		Mole Ratios	Unit Cell Formulae	Unit Formula Weight	Density g.ml ⁻¹
	SiO ₂	Na ₂ O	M ₂ O ₃	R ₂ O	H ₂ O				
ZA-1	85.72	1.011	1.65	7.56	4.06	44.14	Na _{2.12} (Al _{2.12} Si _{93.87} O ₁₉₂) TBA _{1.92} 14.82 H ₂ O	5816.73	1.164±0.35
ZA-2	86.45	0.65	1.052	7.51	4.35	69.82	Na _{1.37} (Al _{1.36} Si _{94.64} O ₁₉₂) TBA _{1.96} 15.87 H ₂ O	5799.08	1.824±0.42
ZA-3	87.25	0.215	0.351	7.83	4.42	211.14	Na _{0.456} (Al _{0.452} Si _{95.54} O ₁₉₂) TBA _{2.01} 16.13 H ₂ O	5778.09	1.864±0.25
ZF-1	88.15	0.622	1.605	7.27	2.35	73.22	Na _{1.29} (Fe _{1.29} Si _{94.7} O ₁₉₂) TBA _{1.58} 8.41 H ₂ O	5833.08	1.911±0.12
ZF-2	89.56	1.181	3.05	4.61	1.15	39.15	Na _{2.385} (Fe _{2.39} Si _{93.6} O ₁₉₂) TBA _{1.15} 4.0 H ₂ O	5809.98	1.964±0.75
ZF-3	89.11	1.204	3.11	4.51	2.10	38.20	Na _{2.44} (Fe _{2.44} Si _{93.55} O ₁₉₂) TBA _{1.13} 7.342H ₂ O	5890.06	2.011±0.08

M = Al or Fe

materials. It is observed that a high silica zeolite synthesis system is formed in which a minor amount of structure-directing agent is used to specify the nucleation product, and then a larger amount of an amine (TBA) is used to provide both pore filling and basicity capacities in the synthesis. It is also observed that the synthesis conditions, such as pH, temperature, time, and sources of silica influenced the densities and other physico-chemical properties of zeolite materials. The pH in the synthesis mixture is governed by the presence of OH^- ions. Raising pH of synthesis mixture using OH^- , mainly influence the crystallization of zeolite in a positive way within the synthesis field. The OH^- is a strong mineralization agent for bringing reactants into solution. The higher the pH more the rate of crystal growth of zeolite materials. [19]

3.2. Thermal analysis

Results of TG-DTA derivato-graphic of as synthesized zeolite-type materials (ZA-3 & ZF-3) are presented in Fig. 2 which shows the general character of TG-DTA curves. Identical thermal effects were observed to occur during the heat treatment but the oxidation proceeds in stages and the organic cations were removed from aluminosilicate based on iron and aluminium contents. In temperature range (100-750 °C) the form of TG/DTA curves of ferrosilicate and aluminosilicate materials were identical, attesting to the identical nature of processes occurring in them during heating in air. It is observed from the TG/DTA curves that the as-synthesized products (ZA-3I & ZF-3) have one main thermal effect approx. at (350-510 °C) and this main thermal effect is assigned to the decomposition of organic template molecules ($\text{C}_3\text{H}_7)_4\text{N}^+ = \text{TBA}^+$) as well as framework water and /or structural hydroxyl group. The sorbed water and possibly part of organic molecules located and bound within the zeolite skeleton, which amount to 3-3.5% of the weight of the specimen. The ~6-8% weight loss associated with removal of the TBA^+ cation. The identical nature of oxidation processes of the TBA^+ cations stabilized in the structures of the ZSM11-Al and ZSM11-Fe allows us to postulate that the sites for the cations in them are identical and the volume of the cages and channels are approximately equal and such type of results were confirmed by the x-ray diffraction patterns. The observed average values of 3 to 4 TBA^+ per unit cell of 96 SiO_2 for

ZSM11-Al and ZSM11-Fe are in agreement with the previous observation [20].

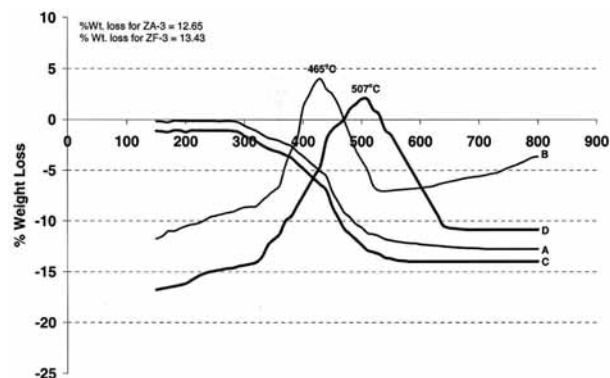


Figure 2. TG/DTA curves for selected specimens of aluminium-deficient and ferrosilicate zeolite-type materials. A = TG for ZSM11-Al B= DTA for ZSM11-Al C = TG for ZSM11-Fe D= DTA for ZSM11-Fe.

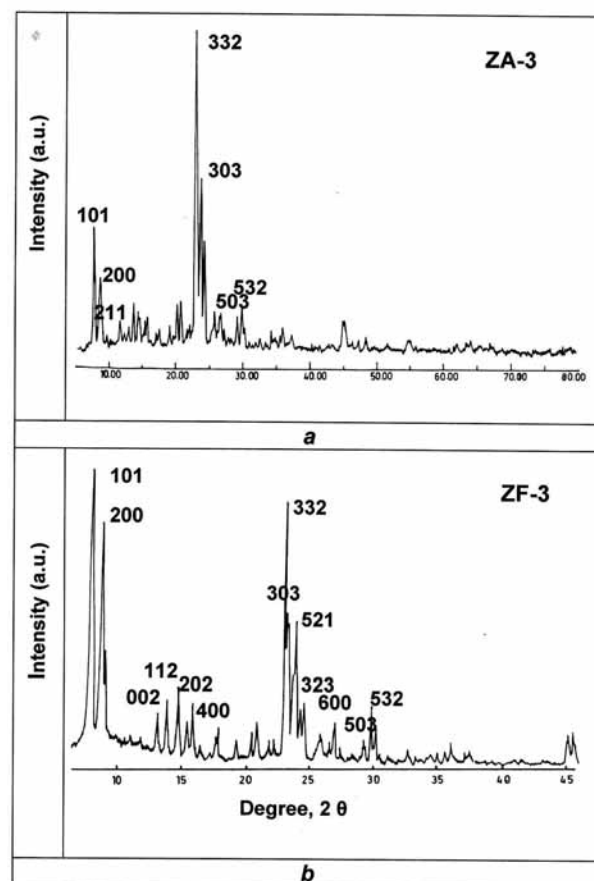


Figure 3 (a-b). X-ray diffraction patterns of selected specimens (a) ZA-3 and (b) ZF-3.

3.3. X-Ray Diffraction

From the analysis of the dry product by diffraction of X-rays, some selected aluminium-deficient and their analog zeolite-type materials specimens i.e. ZA-3 and ZF-3 were used for determination of percentage crystallinity. Peak positions and relative intensities of X-ray diffraction patterns are shown in Fig. 3 (a-b). Intensity of diffraction peaks were used to determine the degree of crystallinity of the synthesized materials.

A quantitative measure of the crystallinity of a molecular sieve material is made by using the summed heights of approximately eight peaks in the X-ray diffraction pattern. The approximate degree of crystallinity is given by the ratio of peaks areas corresponding to the crystalline phase (selected over the range: $18.5^\circ < 2^\circ < 31^\circ$) to the sum of the areas of the crystalline phase and the amorphous phase [21-22]. The relative crystallinity was calculated quantitatively by comparing the sum of the peak heights of the unknown material divided by the sum of the peaks heights of a standard sample.

$$\% \text{Crystallinity} = \frac{\sum \text{Peak heights of unknown product}}{\sum \text{Peak heights of known material}} \times 100$$

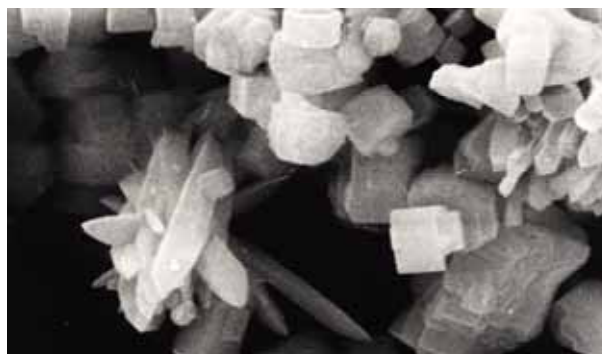
$$\% \text{Crystallinity} = \frac{\text{Peak area of } 2\theta = 22 - 25^\circ \text{ of unknown}}{\text{Peak area of } 2\theta = 22 - 25^\circ \text{ of known}} \times 100$$

X-ray diffraction is a useful technique for measuring maximum crystallite sizes of $\sim 300 \text{ \AA}$ at large angles; the limit is 100 \AA with medium angles. The width of the diffraction peaks gives information about the mean crystallite size of the material. The mean crystallite size was calculated using the classical Debye-Scherrer equation as follows :

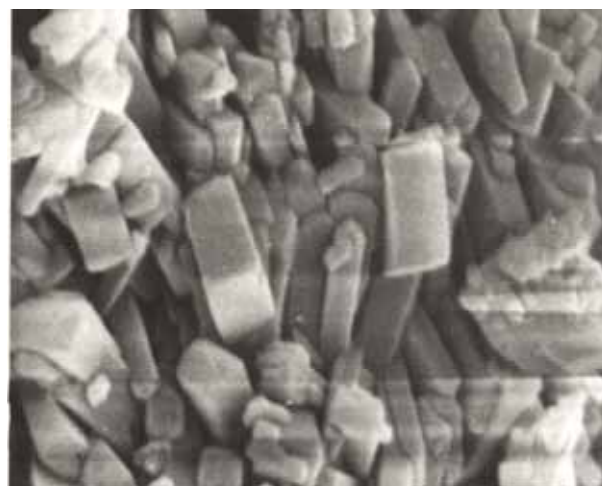
$$L(\text{nm}) = \frac{K\lambda(\text{nm})}{B\cos\theta}$$

Where L is the average crystal size in the direction of the d spacing, K is a shape constant (assumed as 1), λ wavelength of the radiation used (0.1541 nm for CuK_α), β is the full width at half-maximum (FWHM) of the selected peaks of materials. θ is the diffraction peak angle measured in radians. The average crystallites size and crystallinity (96-98%) of synthesized products were presented

in Table 3. The crystallinity data showed that the synthesized materials are highly crystalline.



(a) ZA-1



(b) ZA-2



(c) ZA-3

Figure 4(a-c). Scanning electron micrographs of aluminum-deficient zeolite-type materials.

Table 3. XRD, SEM and PSA analysis.

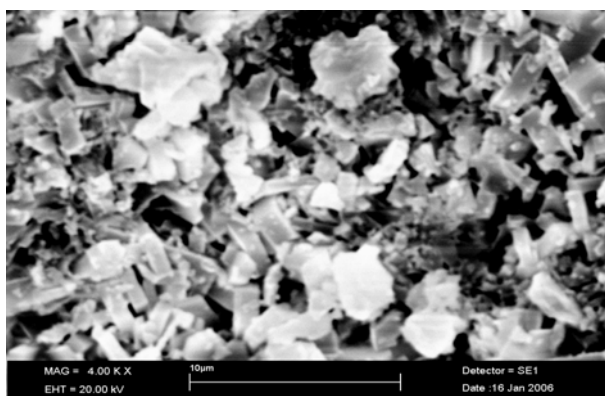
Specimens	XRD Analysis					SEM		PSD
	Crystallinity %	Unit cell parameters (Å)			Unit cell volume (Å) ³	Crystals Shape	Particle Size (µm)	Median Particle Size (Microns)
		a	b	c				
ZA-1	92.15±.42	20.11(2)	20.11(2)	13.44(1)	5435	Cylindrical	5.67-8.95	56.31
ZA-2	94.35±.81	20.15(3)	20.15(3)	13.35(2)	5420	Intergrowth Rod-like	2.25-3.15	58.02
ZA-3	98.36±.6	20.12(2)	20.12(2)	13.48(2)	5456	Rectangular	1.85-2.65	60.42
ZF-1	90.42±.35	20.08(3)	20.08(3)	13.36(3)	5386	Cylindrical tube-like	4.5-7.5	38.12
ZF-2	95.47±.64	20.06(2)	20.06(2)	13.29(1)	5348	Twinned cylindrical	1.80-3.1	41.26
ZF-3	99.5±.45	20.02(3)	20.02(3)	13.05(2)	5230	Twinned cylindrical	1.50-2.25	43.20

Tetragonal unit cell volume = a^2c Unit cell parameter $a=b \neq c$, PSD = Particle size distribution Median = $\frac{1}{2} [n/2 + (n/2+1)]$.

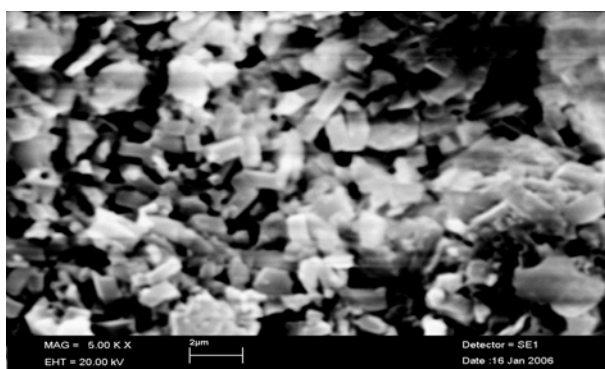
All the relatively sharp peaks were indexed using unit cell refinement and least squares programme, ITO software [23]. The unit cell parameters and volume were obtained by a least square fit of the interplaner spacing of 6-8 strong reflections occurring in step scanning procedure with the step 0.02° . The refined unit cell parameters, volume and symmetry of synthesized products are presented in Table 3. Peak position and relative intensities of XRD pattern indicates that the selected synthesized products ZA-3 and ZF-3 were tetragonal crystal. The cell parameters and unit cell volume of specimen ZA-3 were found $a = 20.12 \text{ \AA}$, $b = 20.12 \text{ \AA}$, $c = 13.48 \text{ \AA}$, 5456 \AA^3 , and of specimen ZF-3 are $a = 20.02 \text{ \AA}$, $b = 20.02 \text{ \AA}$, $c = 13.05 \text{ \AA}$, 5230 \AA^3 respectively. The substitution of Al for Fe leads to a slight decrease of three parameters and unit cell volume. These values were further confirmed by comparison the reported values (JCPDS No.42-0022). The unit cell parameters were found to be analogous to those of ZSM5 and ZSM11 [24-25].

Figs. 4–5 indicate that the crystals of aluminosilicate and ferrosilicate zeolite-type materials show well developed faces and appeared as irregular highly twinned cylindrical aggregates. Some crystals have two parts symmetrically related to one another. These are named as twinned crystals. By

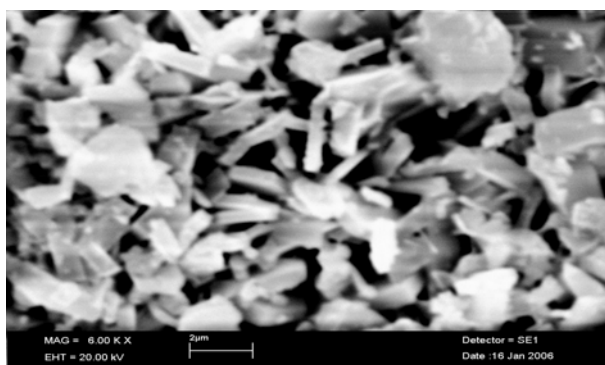
varying the synthesis conditions for both aluminosilicate and ferrosilicate zeolites (e.g., temperature, $\text{SiO}_2/\text{TBA}^+$ and $\text{SiO}_2/\text{H}_2\text{O}$ ratios, and pH of solution) leads to changes in the crystal shape. Fig. 4 and Fig.5 revealed that some rod-like crystals are growing from the large cylindrical aggregate crystal (Fig. 4a) and (Fig. 5a) which indicate that crystal growth mechanism of specimen ZA-1 and ZF-1 are asymmetrical. It is evident that the stoichiometric relationship of metal cations (Al or Fe) and SiO_2 were not feasible for formation of fine ovate and rod-like crystals. Modification of synthesis parameters i.e., pH, temperature, concentration of SiO_2 , and metal cations produced elongated rod-like and ovate-type crystals in specimens ZA-2&3 (Fig. 4 b&c) and ZF-2&3 (Fig. 5 b&c). Erdem et al. [26] has reported crystal morphology of ZSM11-Al as ovate to a maximum dimension of $3 \mu\text{m}$. It appeared that the crystal growth mechanism of specimens ZA-2&3 and ZF-2&3 was very close to the zeolite ZSM11 and influenced by pH, temperature, concentration of SiO_2 , the metals cations (Al or Fe) and independent of the concentration of organic template (TBA^+). However, the main influence in the shape of crystals seems to be the concentration of SiO_2 .



(a) ZF-1



(b) ZF-2



(c) ZF-3

Figure 5(a-c). Scanning electron micrographs of ferrosilicate zeolite-type materials.

The higher the concentration of SiO_2 , i.e., the more the crystallization occurs in a dense gel, the more the elongated forms is reduced [27]. The particle sizes of these crystals were measured point to point method using SEM technique and the results were presented in Table 3. SEM was easily used for the measurement of particle size because it is the most versatile technique and has been used

extensively to examine surface topography and the exact particle size of synthetic zeolite materials. Particle size results were found 5% significant level with certain minor errors [28-39].

The particle size distribution shown in percent histogram of Fig. 6 indicated that the median diameter of particles for aluminio-deficient and ferrosilicate zeolites were in the range of 56~60 and 38~43 microns respectively. The particle size distribution of silica particles prepared by rice husk is ~30 microns. These results revealed that substitution of Al for Fe leads to decrease of particle size distribution and depending on the hydrothermal crystallization time. Thus particle size distribution gradually became broader and approached an asymptotic value as the crystallization process increased.

Conclusions

- Hydrothermal synthesis of aluminium-deficient and ferrosilicate zeolite-type materials depends mainly upon $\text{SiO}_2/\text{M}_2\text{O}_3$ mole ratios, time, temperature, pH and types of organic templates. Substantial reduction in synthesis time i.e., 3 days, was achieved by crystallization of zeolite materials ZSM11-type with hydrothermal synthesis at elevated temperature of 170 °C in an alkali system.
- Well-selected physical methods i.e., TG/DTA, XRD and SEM allowed discriminating between aluminio- and ferrosilicate zeolite type materials. TG/DTA provided the knowledge of incorporation of organic template ion TBA^+ near the theoretical limit of two molecules per unit cell for ZSM11 type materials whereas XRD indicated the phase purity of ZSM11-type structure and subsequently the use of peak index method confirmed the unit cell parameters and unit cell volume. Scanning electron microscope examination showed their degree of crystallinity and diagnostic crystalline morphology. The crystallinity of a desired zeolite phase can also be improved by the choice and amount of inorganic cation used in the synthesis gel. DTA thermogram did not indicate any high temperature exothermal characteristic of lattice breakdown at least up to 600 °C. This indicates that the synthesized zeolite-type materials were thermally stable and structurally stable at least upto 550 °C.

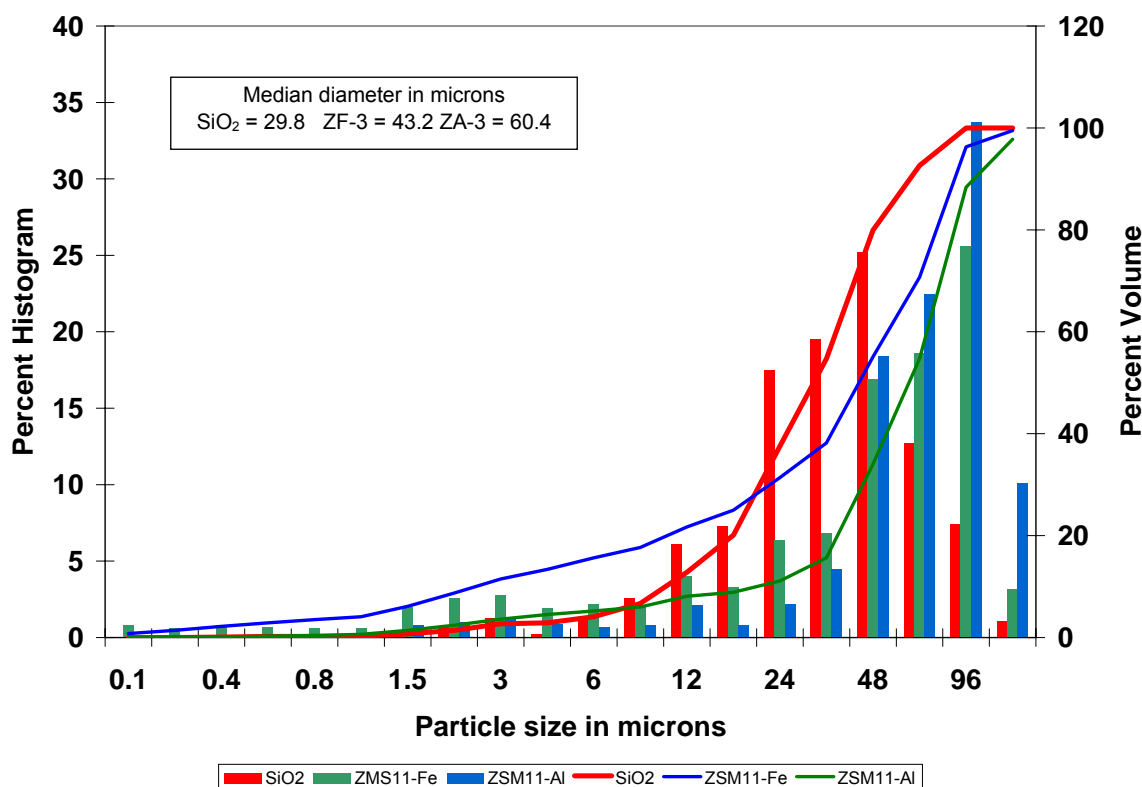


Figure 6. Particle size distribution of some selected specimens of rice husk silica, aluminium-deficient and ferrosilicate zeolite-type materials.

- Calcination of zeolite materials to decompose and remove templates effectively was achieved by heating the materials in air flow for 8h at 550 °C. Calcination of zeolite has no significant effect on crystallinity.

References

- [1] J., Karge, H. G., Pfeifer, H., Holderich, W., Eds. *Zeolites and Related Microporous Materials: State of the Art*, Weitkamp, Elsevier Amsterdam, (1994).
- [2] M. M.J. Treacy, B. K. Marcus, M. E. Bisher and J.B. Higgins, Eds., *Materials Research Society: Warrendale, PA*, (1999).
- [3] Sh. Sang, F. Chang, Zh. Liu, Ch. He, Y. He and L. Xu, *Catal. Today* **93** (2004) 729.
- [4] L. Shirazi, E. Jamshidi and M. R. Ghasemi, *Cryst. Res. Technol.* **43** (2008) 1300.
- [5] R. Szostak, *Handbook of Molecular Sieves*; Van Nostrand: New York, (1992).
- [6] R. M. Mohamed, H. M. Aly, M. F. El-Shahat, I.A. Ibrahim, *Microporous and Mesoporous Materials* **79** (2005) 7.
- [7] P. Pookmanee, G. Rujijanagul, S. Ananta, R.B. Heimann and S. Phanichphant, *J. Eur. Ceram. Soc.* **24** (2004) 517.
- [8] M. P. Roxana, *Nanotechnology* **14** (2003) 312.
- [9] M. Zhang, Z. S. Jin, J. J. Yung and Z. J. Zhang, *J. Molec. Catal. A: Chem.* **217** (2004) 203.
- [10] C.E.A , Kirschock, R. Ravishankar, P. A. Jacobs and J. Martens, *J. Phys. Chem. B* **103** (1999) 11021
- [11] D.P. Serrano and S. Van Grieken, *J. Mater. Chem.* **11** (2001) 2391.
- [12] O. Terasaki, T. Ohsuna, Z. Liu, Y. Sakamoto and A.E. Garcia-Bennett, *Studies in Surface Science and Catalysis, 148 (Mesoporous Crystals and Related Nano-Structured Materials)*, (2004) 261.

- [13] Y. Sasaki and H. Kato, *Zeolites* **21** (2004) 1.
- [14] M. Patal and A. Karera, *J. Mater. Sci. Lett.* **8** (1989) 955
- [15] H.H. Willard, L.L.Jr. Merrit, J.A. Dean and F.A. Jr. Settle, *Instrumental methods of analysis*, 7th Ed., Wadsworth Publishing Company, USA, (1988).
- [16] American Society for Testing and Materials (ASTM), *Annual Book of ASTM Standards*, Section 15.02 C169-80, (1987).
- [17] A.I. Vogel, *Text book of quantitative chemical analysis*, G.H. Jeffery, J. Bassett, J. Mendham and R.C. Denney (Eds.), Longman Scientific and Technical Ltd., Essex-England, (1989).
- [18] G.T. Kokotailo, P.Chu and S.L. Lawton, *Nature* **275** (1978) 199.
- [19] D.T.Hayhurst, A.Nastro, R.Aiello, F.Crea and G. Giordano, *Zeolites* **8** (1989)416
- [20] D. Zhao, Sh. Qiu and W. Pang, *Zeolites* **13** (1993) 478.
- [21] N. Kumar, V. Nieminen, K. Demirkan, T. Salmi, D. Y. Murzin and E. Laine, *Appl. Catal. A* **235**, (2002) 113.
- [22] L. D. Rollmann, "Synthesis of zeolites, an overview, *Zeolites: Science and Technology*", Martinus Nijhoff Publishers, Hague, (1984) p. 109.
- [23] J. W. Visser, *J. Appl. Crystallogr.* **2** (1969) 89
- [24] JCPDS No.42-0022 (2002), International Centre for diffraction data.
- [25] R.H. von Ballmoos, *J. Collection of Simulated XRD powder pattern for Zeolites* **10** (1990) 4365
- [26] A. Erdem and L.B. Sand, In *Proc. 5thInt. on Zeolite Conf.*, ed. J.V.C. Rees. Heyden, London, (1980).
- [27] P.A. Jacobs and J.A. Martens, *Stud. Surf. Sci. Catal.* **33** (1987) 71.
- [28] S. K. Durrani, N. A. Chughtai, J. Akhtar, K. Saeed, M. Arif and M. Ahmed, *The Nucleus* **37** (2000) 35.
- [29] S. K. Durrani, J. Akhtar, N. A. Chughtai, M. Ahmad and M.J. Moughal, *J. Mat. Sci. Tech.* **21**, Nos. 4 (2005) 563.

